

THE SORPTION AND PERMEATION OF CO₂ AND CH₄ FOR DIMETHYLATED POLYSULFONE MEMBRANE

Hyun-Joon Kim and Suk-In Hong[†]

Department of Chemical Engineering, Korea University,
1, 5-ka, Anam-dong, Sungbuk-ku, Seoul 136-701, Korea
(Received 31 August 1996 • accepted 23 May 1997)

Abstract – The sorption and permeation properties of the CO₂ and CH₄ were measured for polysulfone and dimethylated polysulfone to investigate the structure-property relationships. The effect of operating pressure on the transport properties of the polysulfones was examined. The permeation properties for a mixture of CO₂ and CH₄ (CO₂/CH₄=57.5/42.5 vol%) were also measured and these results were compared with those obtained from the experiments of pure gases. The sorptions of CO₂ and CH₄ are well described by "dual-sorption model". The permeability coefficients of CO₂ and CH₄ decreases with increasing upstream pressure, as is often the case with other glassy polymers. The permeability coefficients of each gas of binary mixture are reduced than those for pure gases. This result is due to the competition of each gas for the Langmuir sites. The free volume of the dimethylated polysulfone is lower than that of polysulfone, and dimethylated polysulfone shows relatively lower permeability coefficients and higher selectivity than polysulfone.

Key words: Dimethylated Polysulfone, Sorption, Permeation

INTRODUCTION

Over the past decade, gas separation using membranes have emerged as an important alternative operation to cryogenic distillation or pressure swing adsorption. New materials with higher permeability and selectivity are required to advance membrane technology in the commercial areas. In general, so called "trade-off" exists between permeability and permselectivity among polymers that are used as membranes [Pixton and Paul, 1994]. Careful molecular design of polymer structure can lead to materials that can run counter to a certain extent the trade-off relationships. Recent studies have been focused at systematically varying polymer structure to increase permeability without decreasing selectivity, or to enhance selectivity without loss of permeability [McHattie et al., 1991; Kim et al., 1988; Houde et al., 1995; Tanaka et al., 1992; Aitken et al., 1992]. Structural changes that inhibit chain packing can increase permeability and those that reduce intramolecular mobility around flexible linkages in the polymer backbone can lead to higher selectivity. Simultaneous suppression of intersegmental packing and intramolecular mobility can yield increase in both permeability and selectivity [Cotello and Koros, 1994].

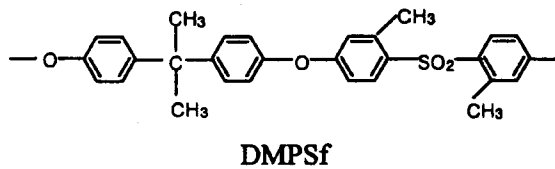
This present work involves the synthesis of dimethylated polysulfone in which ortho sites of sulfone unit in polysulfone have been replaced with methyl substituents. The gas pair chosen for this study is the CO₂/CH₄ system. The separation of these gases is of interest in oil recovery, the treatment of landfill gases and sweetening of natural gases [Bhide and Stern, 1993; Bollinger et al., 1982; Rantenbach, 1994]. It is the purpose of this study to investigate the effect of feed pressure on the permeation properties, and to examine the effect of the substituent on CO₂/CH₄ transport properties that are important for candidate

materials for gas separation membranes.

EXPERIMENTAL

1. Synthesis of Dimethylated Polysulfone (DMPSf)

The procedure described by Guiver et al. [1989] was used for the synthesis of dimethylated polysulfone (DMPSf). Polysulfone (PSf, Udel® P-3500, 0.027 mol, 12 g) was dissolved in distilled THF (403 mL) and the temperature of the solution was reduced to below -30 °C. n-Butyllithium (0.06 mol, 6 mL of 10 M in hexane) was added dropwise. The mixture turned a red-brown color. The polymer was methylated after 30 minutes by the dropwise addition of excess iodomethane. The resulting solution was stirred for 1 hr, and then precipitated into isopropanol, washed several times, and finally dried to yield DMPSf.



2. Membrane Preparation

The membranes were cast from 10 wt% solution in methylene chloride on the clean glass plate at room temperature. The membranes were dried under atmosphere for 24 hrs, controlling the rate of solvent removal. After removing from the glass plate, the membranes were completely dried in a vacuum oven at 150 °C for several days.

3. Gas Sorption and Permeation

Pure gas sorption measurements were made for CO₂ and CH₄ up to 20 atm and at 30 °C. Equilibrium sorption was measured by the pressure decay method. The sorption cell is similar to one

[†]To whom correspondence should be addressed.

designed by Koros and Paul [1976].

Permeability measurements were also made for pure CO_2 and CH_4 and their binary mixture using the variable volume method. A schematic diagram of the apparatus for permeability measurement is shown in Fig. 1. Pure gas to permeated was fed into upstream side, while downstream side was filled with the same gas at 1 atm. The volumetric flow rate through the membrane to the downstream side was determined by observing the displacement of isopropanol in the capillary tube connected to the downstream side. The permeability coefficients were calculated by Eq.(1) and (2). Permeation runs were carried out at 30°C and pressures up to 20 atm.

$$P = \bar{D} \cdot \bar{S} = \frac{J_s L}{P_1 - P_2} \quad (1)$$

$$J_s = \frac{\pi d^2}{4A} \frac{273.15 p_b}{76T} \frac{dh}{dt} \quad (2)$$

where P is the mean permeability coefficient, \bar{D} is the apparent diffusion coefficient, S is the apparent solubility coefficient, J_s is the steady-state rate of gas permeation through unit area when the constant gas pressure p_1 and p_2 are maintained at the membrane interface, and L is the effective membrane thickness. And d is the diameter of capillary, A is the membrane permeation area, p_b is the barometric pressure, T is the experimental temperature, and dh/dt is the displacement rate of propanol in the capillary. The permeation rates for the components of binary gas mixture of CO_2 and CH_4 ($\text{CO}_2/\text{CH}_4=57.5/42.5$ vol%) were determined by the volumetric flow rate of gas mixture and the concentrations of each component on the upstream and downstream side. The concentrations of the components were determined by Gas Chromatograph with a column packed with Porapak Q. Permeation runs for the binary mixture were carried out at stage cuts below 0.01.

4. Characterization

¹H-NMR spectra were recorded on a Bruker AM 100 MHz spectrophotometer. Samples were dissolved in CDCl₃ with an internal TMS (tetramethylsilane) standard. Chemical shifts δ are expressed in parts of million (ppm) and are described as singlet (s), doublet (d), or and multiplet (m). The glass transition temperature for each material was measured using a Perkin-Elmer DSC-7 differential scanning calorimeter at a heating rate of 20 °C/min. Polymer densities were measured using a density gradient

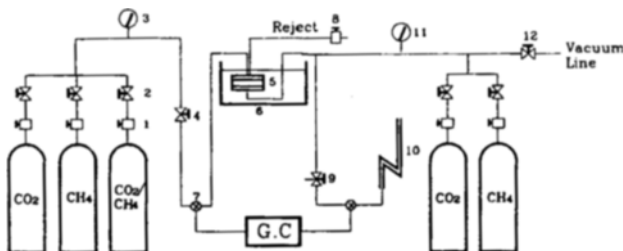


Fig. 1. The experimental apparatus for permeability measurement.

1. Needle valve	7. Sampling port
2. On/Off valve	8. Needle valve
3. Pressure gauge	9. 3-Way valve
4. On/Off valve	10. Capillary
5. Permeation cell	11. Vacuum gauge
6. Water bath	12. On/Off valve

column filled with aqueous solutions of calcium nitrate at 30 °C. Fractional free volumes of the polymers were calculated by a group contribution method proposed by Bondi [Van Krevelen, 1989]. The wide-angle X-ray diffraction (WAXD) measurements were carried out using Cu K α radiation with wavelength of 1.54 Å. The average intersegmental distances or "d-spacings" were calculated from Bragg equation [Balta-Calleja and Vonk, 1989], $n\lambda=2d \sin \theta$, at the angle of maximum peak of scan. Cohesive energy densities were calculated by Fedor's group contribution method.

RESULTS AND DISCUSSIONS

1. Pure Gas Sorption and Permeation

Sorption isotherms for CO_2 and CH_4 in PSf and DMPSf are shown in Fig. 2. For each polymer, the pure gas sorption isotherms show concave to the pressure axis, and can be described by "dual sorption model" [Stannet, 1978]. According to dual sorption model, the equilibrium concentration of sorbed gas in glassy polymers can be described as a function of pressure:

$$C = C_D + C_H$$

$$C = k_D p + \frac{C_H bp}{1+bp} \quad (3)$$

where C is the equilibrium concentration of the sorbed gas, C_D and C_H represent Henry' law mode sorption and Langmuir mode sorption, respectively. The parameter k_D is the Henry's law solubility constant, C'_H is the Langmuir capacity constant, and b is the Langmuir affinity constant. These sorption parameters can be obtained by nonlinear least-square regression, and are listed Table 1. The solid curves in Fig. 2 are calculated by Eq. (3), substituting the values of sorption parameters given in Table 1. The sorbed concentrations are well fitted to dual sorption model. Fig. 3 represents the corresponding plot of apparent solubility coefficient versus gas pressure. The apparent gas solubility coefficients in glassy polymers are decreasing function of pressure as illustrated by Eq. (4), and equal to the secant slope of the sorption isotherms.

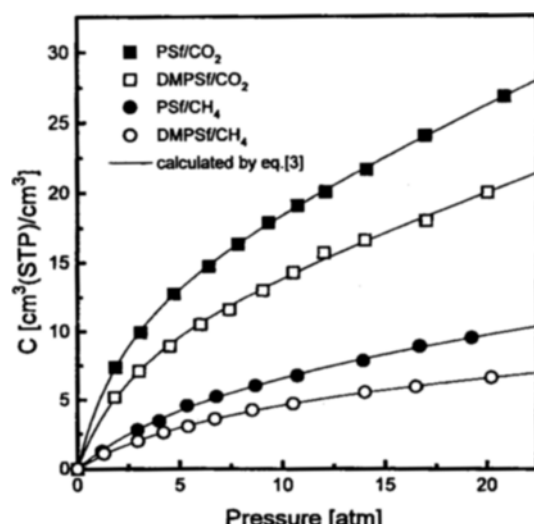


Fig. 2. Sorption isotherms for CO_2 and CH_4 in polysulfone and dimethylated polysulfone at 30 °C.

Table 1. Dual mode parameters of PSf and DMPSf at 30 °C

Polymer	Gas	k_D	C'_H	b	D_D	D_H
PSf	CO_2	0.630	16.503	0.356	4.799	0.581
	CH_4	0.167	9.044	0.118	0.692	0.106
DMPSf	CO_2	0.482	12.166	0.287	2.846	0.452
	CH_4	0.078	7.348	0.108	0.520	0.051

Units: k_D [cm³ (STP)/cm³ atm]; C'_H [cm³ (STP)/cm³]; b (atm⁻¹); D_D × 10 (cm²/s); D_H × 10 (cm²/s)

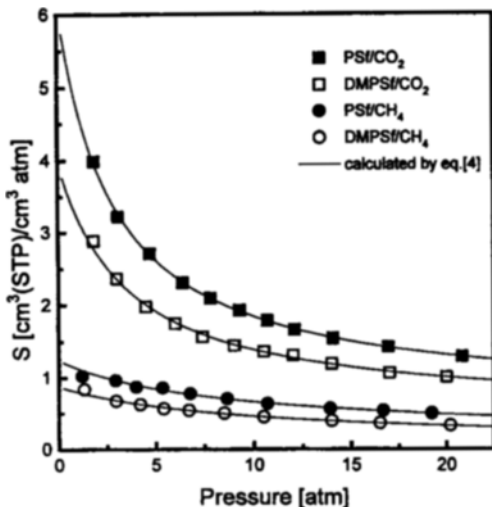


Fig. 3. Pressure dependency of solubility coefficients for CO_2 and CH_4 in polysulfone and dimethylated polysulfone at 30 °C.

$$\bar{S} \equiv \frac{C}{p} = k_D + \frac{C'_H b}{1 + bp} \quad (4)$$

In Fig. 3, the apparent solubility coefficient decreases as the Langmuir sorption sites are saturated, and approaches the asymptotic value of Henry's law solubility constant, k_D . The degree of pressure dependency of solubility coefficients varies with gases and polymers. For each polymer, the greater pressure-dependency of CO_2 solubility coefficient is due to the large value of C'_H for CO_2 compared with that for CH_4 . The difference of pressure-dependency of solubility coefficients between PSf and DMPSf is also due to the difference of the value of C'_H .

Pure gas permeability coefficients of CO_2 and CH_4 for PSf and DMPSf are shown as a function of upstream pressure in Fig. 4 and 5. The permeability coefficients of CO_2 and CH_4 decreases with increasing upstream pressure, as is often the case with other glassy polymers. The decreasing permeability coefficients of CO_2 and CH_4 are attributed to the decreasing function of solubility coefficients as explained by Fig. 3. This pressure-dependency of permeability coefficients can be described as "dual mobility model" (or "partial immobilization model") proposed by Paul and Koros [1976]. According to dual mobility model, the populations in each the sorptions can be assigned separate diffusion coefficients D_D and D_H , the permeability coefficients of pure gas can be written as;

$$P = k_D D_D \left[1 + \frac{FK}{(1+bp_1)(1+bp_2)} \right] \quad (5)$$

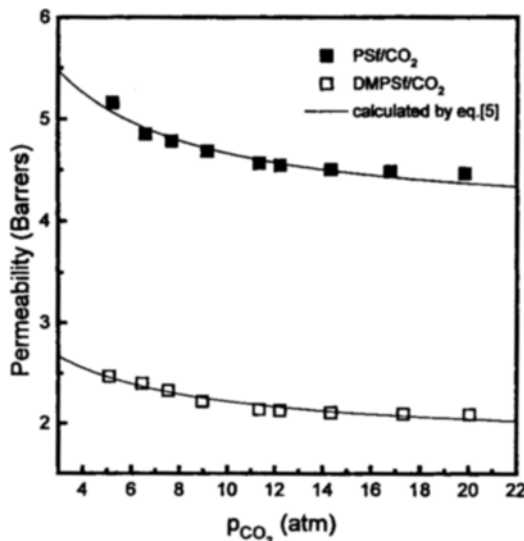


Fig. 4. Permeability coefficients for CO_2 through polysulfone and dimethylated polysulfone at 30 °C.
[1 Barrer=10⁻¹⁰ cm³ (STP) cm/cm² s cmHg]

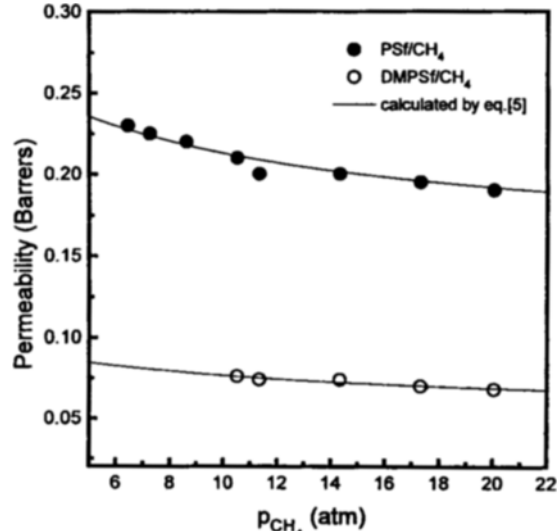


Fig. 5. Permeability coefficients for CH_4 through polysulfone and dimethylated polysulfone at 30 °C.
[1 Barrer=10⁻¹⁰ cm³ (STP) cm/cm² s cmHg]

$$\text{where, } K = \frac{C'_H b}{k_D} \text{ and } F = \frac{D_H}{D_D}$$

The diffusion coefficients, D_D and D_H are calculated from the slope and intercept of the plot of experimental permeability coefficient versus $1/(1+bp_1)(1+bp_2)$. An example of such a plot is shown in Fig. 6 for CO_2 permeation through DMPSf. The diffusion coefficients obtained by this analysis are listed in Table 1. The solid curves in Fig. 4 and 5 are calculated by Eq. (5) using parameters given in Table 1, and show that the permeability coefficients are well fitted to dual mobility model at entire pressure range. In Fig. 4 and 5, the permeability coefficients of gases through PSf are higher than those through DMPSf. This result is discussed below.

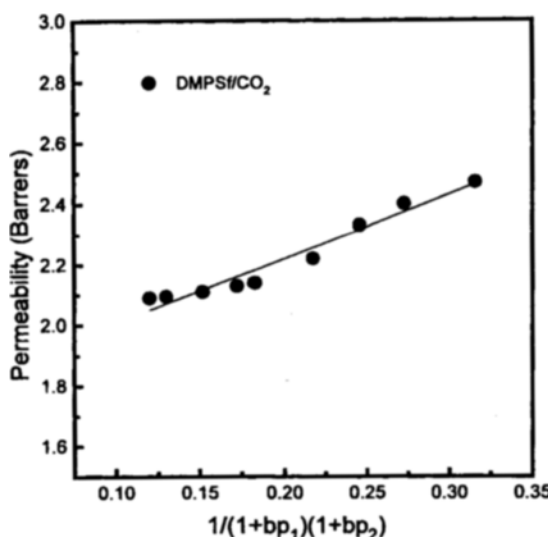


Fig. 6. Correlation of CO_2 permeability coefficient for dimethylated polysulfone with dual mode quantity at 30°C .
[1 Barrer= 10^{-10} cm^3 (STP) $\text{cm}/\text{cm}^2\text{s cmHg}]$

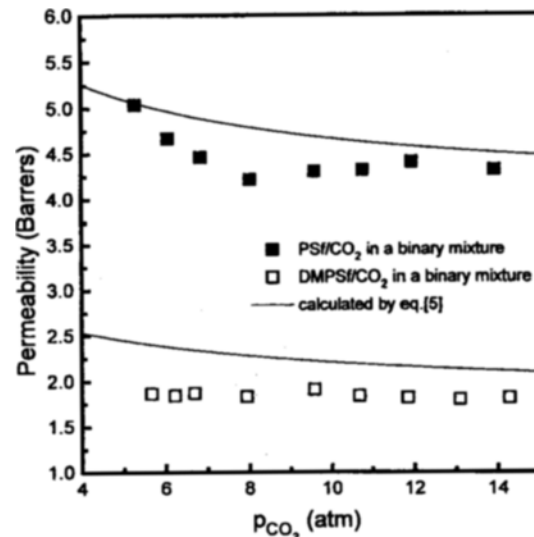


Fig. 7. Permeability coefficients for CO_2 in CO_2/CH_4 mixture (57.5/42.5 vol%) through polysulfone and dimethylated polysulfone at 30°C .
[1 Barrer= 10^{-10} cm^3 (STP) $\text{cm}/\text{cm}^2\text{s cmHg}]$

2. Mixed Gas Permeation

The permeability coefficients of CO_2 in a binary mixture ($\text{CO}_2/\text{CH}_4=57.5/42.5$ vol%) for PSf and DMPSf membranes are illustrated in Fig. 7, and those for CH_4 are shown in Fig. 8. In Fig. 7 and 8, the solid and dashed curves represent values calculated from pure gas data by the dual mobility model [Eq. (5)] based on the respective partial pressures for PSf and DMPSf, respectively. For each polymer, mixed gas permeability coefficients are lower than the respective pure component values. Based on dual sorption model for pure gas, Story and Koros [1989] extended the model to sorption of gas mixtures in glassy polymers. For component A in a binary mixture, the concentration of sorbed gas can be written as Eq. (6).

$$C_A = k_{DA} p_A + \frac{C'_H b_A p_A}{1 + b_A p_A + b_B p_B} \quad (6)$$

where, subscripts A and B represent components A and B, and all the parameters are obtained by pure gas experiment. The Eq. (6) assumed that in the Henry's law mode, solubility, hence, permeability of a given penetrant was independent of the other components present. According to Eq. (6), the above depressions of permeability coefficients in Fig. 7 and 8 result from the competition between CO_2 and CH_4 for the Langmuir sites in glassy polymers. When A and B are relatively noninteracting components, component B fills some of the Langmuir sites previously available to A in the absence of B. The lowering of the concentration driving force of A lowers its flux through the membrane. Therefore, the permeability of A in a binary mixture is lower than that of pure A. In Fig. 7 and 8, the permeability depressions are larger for DMPSf. This result is attributed to lower value of Langmuir capacity constant, C'_H for DMPSf. For each polymer, the depression is larger for CH_4 . This can be explained by the fact that the value of Langmuir affinity constant, b for CO_2 is higher than for CH_4 , so the depression of permeability coefficient of CH_4 in a binary gas mixture is

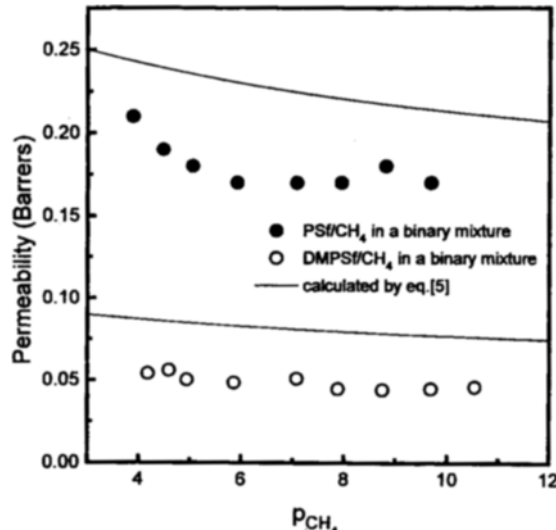


Fig. 8. Permeability coefficients for CH_4 in CO_2/CH_4 mixture (57.5/42.5 vol%) through polysulfone and dimethylated polysulfone at 30°C .
[1 Barrer= 10^{-10} cm^3 (STP) $\text{cm}/\text{cm}^2\text{s cmHg}]$

higher than that of CO_2 , as expected by $b_B p_B$ term in Eq. (6).

The separation factor, α is defined as Eq. (7)

$$\alpha_{(A/B)} \equiv \frac{y_a/y_b}{x_a/x_b} \quad (7)$$

where y 's and x 's are the mole fraction of the components in the downstream and upstream, respectively. When the pressure of the downstream is very small compared with the upstream pressure, the separation factor will be approximately equal to the ratio of permeabilities of pure gases, P_A/P_B , which is called the "ideal separation factor". The solid curves in Fig. 9 correspond to model predictions without considering the competition effect for PSf and DMPSf, ie. ideal separation factors. The result of

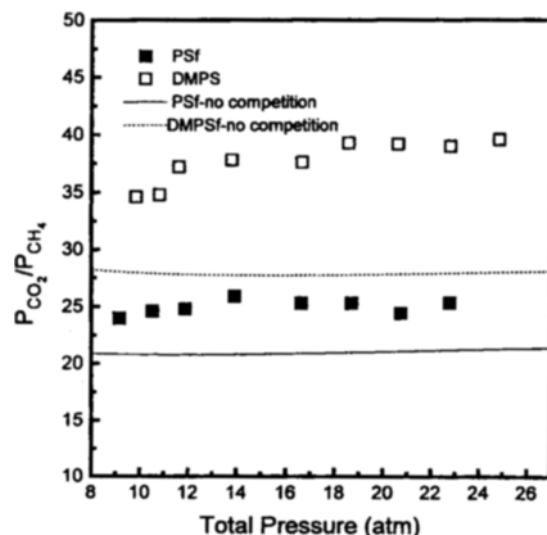


Fig. 9. Ideal separation factors for CO₂ and CH₄ in a binary mixture through polysulfone and dimethylated polysulfone at 30 °C.

separation factors also shows the competition effect between each component. As mentioned above, the depression of permeability coefficient of CH₄ in a binary gas mixture is higher than that of CO₂. Therefore, separation factor is higher than the value without considering competition effect. The difference of ideal separation factor between PSf and DMPSf is discussed at the section below.

3. The Effect of Methyl Substituent on Permeation Properties

Fig. 10 shows the ¹H-NMR spectra of PSf and DMPSf. In the spectrum of DMPSf, the substitution of methyl group is ascertained from the dimethyl singlet at δ=2.30. The detailed analysis for the spectrum of DMPSf was reported at elsewhere [Guiver et al., 1988].

In general, the permeability depends on chain stiffness, intermolecular packing distance, and polymer-penetrant interaction. The glass transition temperature is a pragmatic measure of the stiffness of polymer backbone. Intermolecular packing distance is determined from d-spacing or free volume, and the suppression of intermolecular packing yields increases in permeability. The values of glass transition temperature, d-spacing, density, and fractional free volume for polysulfones are listed in Table 2. The fractional free volume (FFV), given Table 2, is calculated Eq. (8). The group contribution method of Bondi is used to calculate V, hypothetical specific volume of the polymer at 0 K, and V_T, specific volume of the polymer at T, is determined from the polymer density.

$$FFV = \frac{V - V_o}{V} \quad (8)$$

In this study, the permeability coefficients of CO₂ and CH₄ for DMPSf are lower than those for PSf as illustrated in Fig. 4 and 5. As shown in Table 2, DMPSf has lower value of FFV with the similar value of d-spacing in spite of the replacement of phenyl hydrogen of PSf with methyl groups. This results can be explained that the methyl groups of DMPSf are accommodated between the polymer chains without forcing apart them, so that their net effect is decreases in FFV, and consequently in

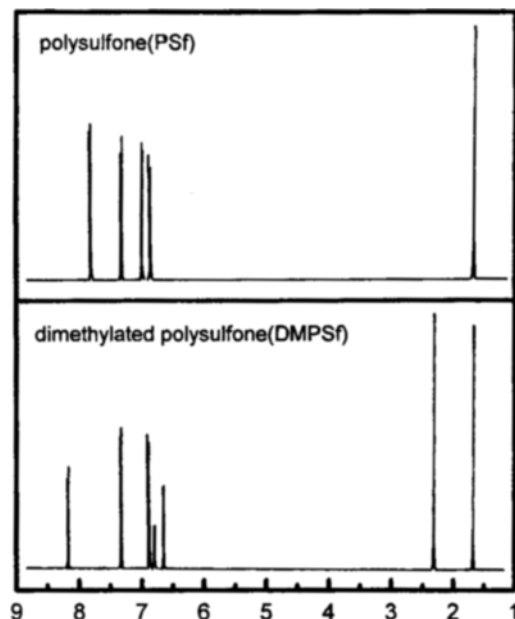


Fig. 10. ¹H-NMR spectra of PSf and DMPSf.

Table 2. Physical properties of PSf and DMPSf

Polymer	T _g (°C)	ρ ¹ (g/cm ³)	d-spacing (Å)	FFV ² (-)	δ ³ (cal/cm ³) ^{1/2}
PSf	190.3	1.243	5.2	0.158	12.4
DMPSf	177.6	1.213	5.2	0.151	12.1

1. density

2. fractional free volume

3. solubility parameter

Table 3. Transport properties of CO₂ and CH₄ for PSf and DMPSf at 30 °C and 10 atm

Polymer	P _{CO₂}	α _{CO₂/CH₄}	S _{CO₂}	S _{CO₂/CH₄}	D _{CO₂}	D _{CO₂/CH₄}
PSf	4.6	21.9	2.4	2.8	1.9	7.8
DMPSf	2.2	29.0	1.8	3.0	1.2	9.6

Units: P × 10¹⁰ [cm³ (STP) cm/s cm² cmHg]; D × 10⁸ (cm²/s); S × 10² [cm³ (STP) /cm³ cmHg]

permeability coefficients. Other researchers reported that asymmetric aryl substitution leaded to the decrease of FFV [Ghosal et al., 1996; McHattie et al., 1991a]. In addition, Ghosal et al. [1996] reported that aromatic rings are activated for rotation (π-flips) about 1,4 axis. These local segmental motions effectively make the free volume to permit activated rotational motion. However, the addition of an aryl substituent inhibit the mobility of these substituted rings, then these rings will be less efficient at making the volume swept out by π-flips.

The glass transition temperature of DMPSf is lower than the value of PSf. One might expect that the polymer with higher T_g might show lower permeability, but it is not the case in this study. In general, the higher the value of T_g, the lower the permeability coefficient for rubbery polymers. While for glassy polymers, no direct correlation is apparent between T_g values and polymer gas transport properties [McHattie, 1991a, 1991b, 1992]. Muruganandam et al. [1987] reported that although group and

segmental motions are very important factors in gas transport in polymers, it is important to note that all motions do not contribute equally to the transport and that there is no strict proportionality between the permeability coefficient and T_g.

A comparison of the permeability coefficients of CO₂ and ideal separation factors for each polymer at 10 atm are shown in Table 3. The diffusivity and solubility contributions to the permeability and ideal separation factor of each polymer are also shown in Table 3. DMPSf is less permeable than PSf, but exhibits higher values of ideal separation factor. The higher separation factor for DMPSf is due to the tightly packed chain segment. Cohesive energy density (CED) has often been used to estimate intersegmental attraction. In general the higher the CED, the higher the forces between polymer chains, and separation factors. In this study DMPSf has a lower CED, but has the higher value of ideal separation factor. This can be explained that the substitution of methyl groups decreases intersegmental attractive force, however methyl groups fill in the void spaces of polymer matrix as mentioned above. The ideal separation factor is the product of diffusivity selectivity and solubility selectivity, the high diffusivity selectivity in this study results in high ideal separation factor.

CONCLUSION

The dimethylated polysulfone (DMPSf) is synthesized, in which ortho sites of sulfone unit in polysulfone (PSf) are substituted with methyl groups. The replacement of phenylene hydrogenes of PSf with methyl groups results in decreases in chain stiffness, as judged by the value of T_g, and decreases in fractional free volume. DMPSf is less permeable than PSf, but exhibits the higher CO₂/CH₄ ideal separation factor. The higher value of ideal separation factor for DMPSf is due to the lower fractional free volume of DMPSf.

For each polymer, the permeability coefficients for each gas of binary mixture (CO₂/CH₄=57.5/42.5 vol%) are lower than the respective values of pure gases. This result can be attributed to the competition effect between CO₂ and CH₄ for the Langmuir sites.

The sorptions and permeations of CO₂ and CH₄ for PSf and DMPSf are well described by dual-mode model. The differences between PSf and DMPSf in permeability and separation factor is mainly depend on the differences in diffusivity and diffusivity selectivity.

NOMENCLATURE

A	: permeation area [cm ²]
b	: Langmuir affinity constant [atm ⁻¹]
C	: concentration of sorbed gas [cm ³ (STP)/cm ³]
C' _H	: Langmuir sorption constant [cm ³ (STP)/cm ³]
D	: diffusion coefficient [cm ² /s]
d	: capillary diameter [cm]
h	: height [cm]
J _s	: steady state diffusion flux [cm ³ (STP)/cm ² s]
k _D	: Henry's law solubility constant [cm ³ (STP)/cm ³ atm]
L	: membrane thickness [cm]
P	: permeability coefficient [cm ³ (STP) cm/cm ² s cmHg]

p	: pressure [atm]
p _b	: barometric pressure [atm]
S	: solubility coefficient [cm ³ (STP)/cm ³ atm]
T	: temperature [K]
t	: time [s]
x	: mole fraction of upstream
y	: mole fraction of downstream
V	: specific volume [cm ³]

Greek Letter

α	: separation factor
----------	---------------------

Subscripts

A	: component A
B	: component B
D	: Henry's law mode
H	: Langmuir mode
1	: upstream face of the membrane
2	: downstream face of the membrane

REFERENCES

Aitken, C. L., Koros, W. J. and Paul, D. R., "Effect of Structural Symmetry on Gas Transport Properties of Polysulfones", *Macromolecules*, **25**, 3424 (1992).

Balta-Calleja, F. J. and Vonk, C. G., "X-ray Scattering of Synthetic Polymers", Elsevier, Amsterdam, 18, 1989.

Bhide, B. D. and Stern, S. A., "Membrane Processes for the Removal of Acid Gases from Natural Gas. II. Effects of Operating Conditions, Economic Parameters, and Membrane Properties", *J. Membrane Sci.*, **81**, 239 (1993).

Bollinger, W. A., MacLean, D. L. and Nayaran, R. S., "Separation Systems for Oil Refining and Production", *Chem. Eng. Progress, Oct.*, 27 (1982).

Costello, L. M. and Koros, W. J., "Effect of Structure on the Temperature Dependence of Gas Transport and Sorption in a Series of Polycarbonates", *J. Polym. Sci., Polym. Phys. Ed.*, **32**, 701 (1994).

Ghosal, K., Chern, R. T., Freeman, B. D., Daly, W. H. and Negulescu, I. I., "Effect of Basic Substituents on Gas Sorption and Permeation in Polysulfones", *Macromolecules*, **29**, 4360 (1996).

Guiver, M. D. and ApSimon, J. W., "The Modification of Polysulfone by Metalation", *J. Polym. Sci., Polymer Letters Ed.*, **26**, 123 (1988).

Guiver, M. D., ApSimon, J. W. and Katowy, O., "Preparation of Substituted Polysulfones through Ortho-Metalated Intermediates", U.S. patent 4,797,457 (1989).

Houde, A. Y., Kulkarni, S. S., Kharul, U. K., Charati, S. G. and Kulkarni, M. G., "Gas Permeation in Polyarylates; Effects of Polarity and Intersegmental Mobility", *J. Membrane Sci.*, **103**, 167 (1995).

Kim, T. H., Koros, W. J., Husk, G. R. and O'Brien, K. C., "Relationship between Gas Separation Properties and Chemical Structures in a Series of Aromatic Polyimides", *J. Membrane Sci.*, **37**, 45 (1988).

Paul, D. R. and Koros, W. J., "Effect of Partially Immobilizing Sorption on Permeability and Diffusion Time Lag", *J. Polym.*

Sci., Polym. Phys. Ed., **14**, 675 (1976).

Koros, W. J. and Paul, D. R., "Design Considerations for Measurement of Gas Sorption in Polymers by Pressure Decay", *J. Polym. Sci., Polym. Phys. Ed.*, **14**, 1903 (1976).

McHattie, J. S., Koros, W. J. and Paul, D. R., "Gas Transport Properties of Polysulphones: 1. Role of Symmetry of Methyl Group Placement on Bisphenol Rings", *Polymer*, **32**, 840 (1991a).

McHattie, J. S., Koros, W. J. and Paul, D. R., "Gas Transport Properties of Polysulphones: 2. Effect of Bisphenol Connector Groups", *Polymer*, **32**, 2618 (1991b).

McHattie, J. S., Koros, W. J. and Paul, D. R., "Gas Transport Properties of Polysulphones: 3. Comparison of Tetramethyl-Substituted Bisphenols", *Polymer*, **33**, 1701 (1992).

Muruganandam, N., Koros, W. J. and Paul, D. R., "Gas Sorption and Transport in Substituted Polycarbonates", *J. Polym. Sci., Polym. Phys. Ed.*, **25**, 1999 (1987).

Pixton, M. R. and Paul, D. R., "Polymeric Gas Separation Membranes", Paul, D. R. and Yampol'skii, Y. P., eds., CRC press, Boca Raton, 83, 1994.

Rantenbach, R. and Welsch, K., "Treatment of Landfill Gas by Gas Permeation-Pilot Plant Results and Comparison to Alternatives", *J. Membrane. Sci.*, **87**, 107 (1994).

Stannet, V. T., "The Transport of Gases in Synthetic Polymeric Membranes-An Historic Perspective", *J. Membrane. Sci.*, **3**, 97 (1978).

Story, B. J. and Koros, W. J., "Comparison of Three Models for Permeation of CO_2/CH_4 Mixtures in Poly(phenylene oxide)", *J. Polym. Sci., Polym. Phys. Ed.*, **27**, 1927 (1989).

Tanaka, K., Kita, H., Okano, M. and Okamoto, K., "Permeability and Permsselectivity of Gases in Fluorinated and Non-fluorinated Polyimides", *Polymer*, **33**, 585 (1992).

Van Krevelen, D. W., "Properties of Polymers", Elsevier, Amsterdam, 71, 1989.